



Sharif University of Technology  
**Scientia Iranica**  
*Transactions B: Mechanical Engineering*  
 www.scientiairanica.com



## Two-phase natural convection of SiO<sub>2</sub>-water nanofluid in an inclined square enclosure

M. Alinia<sup>a,\*</sup>, M. Gorji-Bandpy<sup>a</sup>, D.D. Ganji<sup>a</sup>, S. Soleimani<sup>b</sup>, E. Ghasemi<sup>b,c</sup>  
 and A. Darvan<sup>d</sup>

a. *Department of Mechanical Engineering, Babol University of Technology, Babol, P.O. Box 484, Iran.*

b. *Department of Mechanical and Materials Engineering, Florida International University, Miami, FL 33199, USA.*

c. *Department of Mechanical Engineering, University of Idaho, 1776 Science Center Dr, Idaho Falls, ID 83402, USA.*

d. *Institute of Mechanical Process Engineering, Martin Luther University, Halle-Wittenberg 06099 Halle (saale), Germany.*

Received 7 August 2012; received in revised form 11 February 2014; accepted 15 April 2014

### KEYWORDS

Nanofluids;  
 Two-phase mixture  
 model;  
 Natural convection;  
 Inclination angle;  
 Enclosure.

**Abstract.** Natural convection of a nanofluid consisted of water and SiO<sub>2</sub> in a square enclosure cavity have been studied numerically. The sidewalls are maintained at different constant temperatures and the other walls are thermally insulated. Two-phase mixture model has been used to investigate the hydrodynamic and thermal behaviors of the nanofluid for various inclination angles of enclosure ranging from  $\theta = -60^\circ$  to  $\theta = 60^\circ$ , for Rayleigh numbers varying from  $10^3$  to  $10^7$  and for volume fraction  $\phi = 0 - 6\%$ . The governing equations in a two-dimensional space are solved numerically using the finite-volume approach. The results show that the average Nusselt number increases with growth of both Rayleigh number and the volume fraction of the nanoparticles. Moreover, inclination angle can be a control parameter for nanofluid filled enclosure, and the angle, in which the maximum average Nusselt number occurs for various values of Rayleigh numbers and volume fraction, is obtained.

© 2014 Sharif University of Technology. All rights reserved.

### 1. Introduction

Nanotechnology has been widely used in industry as materials with the size of nanometers possess unique physical and chemical properties. It aims at manipulating the structure of matter at the molecular level with the goal of innovation in every industrial and public endeavor, including physical sciences, electronics cooling, biological sciences, transportation, the environment and national security. The low thermal conductivity of conventional heat transfer fluids, such as water, oil, and ethylene glycol mixtures, is a serious limitation in improving the performance and compactness of engineering equipment. To overcome this disadvantage, there is strong motivation to develop advanced heat

transfer fluids with substantially higher conductivity. One way is to add small solid particles in the fluid. The main idea supports Maxwell's study [1]. He showed the possibility of increasing the thermal conductivity of a fluid-solid mixture by more volume fraction of solid particles. Particles with micrometer or even millimeter dimensions are used. By improving the technology to make particles in nanometer dimensions, a new generation of solid-liquid mixtures, called nanofluid, has appeared. Nanofluids are a new kind of heat transfer fluid containing small quantities of nano-sized particles (usually less than 100 nm), which are uniformly and stably suspended in a liquid. The dispersion of a small amount of solid nanoparticles in conventional fluids changes their thermal conductivity remarkably. Choi [2] quantitatively analyzed some potential benefits of nanofluids. Xuan and Roetzel [3] identified two causes of improved heat transfer by

\*. *Corresponding author. Tel./Fax: +98 111 3234205  
 E-mail address: Alinia\_378@yahoo.com (M. Alinia)*

nanofluids: increased thermal dispersion due to the chaotic movement of nanoparticles that accelerates energy exchanges in the fluid, and the enhanced thermal conductivity of nanofluids. Kelbinski et al. [4] studied four possible mechanisms that contribute to the increase in nanofluid heat transfer: The Brownian motion of the particles, molecular-level layering of the liquid/particle interface, heat transport in the nanoparticles, and nanoparticle clustering. Wen and Ding [5] focused on the entry region under a laminar flow condition using nanofluids for various concentrations. It is shown that the enhancement increases with the Reynolds number, as well as the volume concentration of the nanoparticle. In a comparison between particle sizes, it is observed that nanofluid with smaller particles shows higher heat transfer coefficient than that with larger particles [6]. Incorporating a dispersion model similar to that for flow through porous media, Khanafer et al. [7] presented a two-dimensional numerical simulation of the natural convection of nanofluids in a vertical rectangular enclosure. Abu-Nada and Oztop [8] studied the effects of inclination angle on natural convection in enclosures filled with Cu-water nanofluid. Ho et al. [9] argued that the enhancement or mitigation of heat transfer depends on the formulas used for the thermal properties for nanofluids. Even though the structure, shape, size, aggregation and anisotropy of the nanoparticles, as well as the type, fabrication process, particle aggregation and deterioration of nanofluids, are important factors in a comprehensive nanofluid modeling study, many researchers still find the classical models to be appropriate for predicting the physical properties of nanofluids [10–12]. Santra et al. [13] studied heat transfer augmentation in a differentially heated square cavity using copper-water nanofluid. Ghasemi and Aminossadati [14] studied natural convection heat transfer in an inclined enclosure filled with a water-CuO nanofluid. They indicated that the inclination angle has a significant impact on the flow and temperature fields and the heat transfer performance at high Rayleigh numbers. Recently, Alinia et al. [15] numerically studied the mixed convection of SiO<sub>2</sub>-water nanofluid in an inclined two sided lid driven cavity using a two-phase mixture model. They indicated that nanoparticles are able to change the flow pattern of a fluid. Besides, they also showed that using a two-phase mixture model gives significant information about the distribution of nanoparticles in a flow field. Convective heat transfer with nanofluids can be modeled using the two-phase or single phase approach [16–18]. The first provides the possibility of understanding the functions of both the fluid phase and the solid particles in the heat transfer process. The single phase approach assumes that the fluid phase and particles are in thermal equilibrium and move with the same velocity, so, it is simpler and requires less

computational time. Ding and Wen [19] showed that particle concentration could only be assumed uniform if the corresponding Peclet numbers are always less than 10. This means that the slip velocity between the fluid and particles may not be zero [20]. Therefore, it seems that the two-phase approach is a better model to apply to nanofluid [21,22]. The main aim of the present paper is to analyze, numerically, the problem of natural convection in a square inclined cavity filled with SiO<sub>2</sub>-water nanofluid using a two-phase mixture model. The flow fields, temperature distributions, rate of heat transfer and distribution of nanoparticles will be presented graphically.

## 2. Problem definition and mathematical model

Natural convection of a nanofluid consisting of water and SiO<sub>2</sub>, which has been studied in a square inclined cavity, is shown in Figure 1. The sidewalls are heated and cooled at constant temperatures,  $T_h$  and  $T_c$ , while the other walls are thermally insulated. The computational results are obtained for inclination angles ranging from  $\theta = -60^\circ$  to  $60^\circ$  and Rayleigh number varying from  $10^3$  to  $10^7$ . The Prandtl number of the base fluid (water) is 6.2, and the nanoparticle volume fraction,  $\phi$ , was, variably, 0%, 2%, 4% and 6%. The corresponding thermophysical properties of the fluid and solid phases (nanoparticles) are shown in Table 1.

## 3. Mathematical formulation

The mixture model, based on a single fluid two-phase approach, is employed in the simulation by assuming that the coupling between phases is strong, and particles closely follow the flow. The two phases are assumed to be interpenetrating, meaning that each phase has its own velocity vector field, and within any control volume, there is a volume fraction of the primary phase

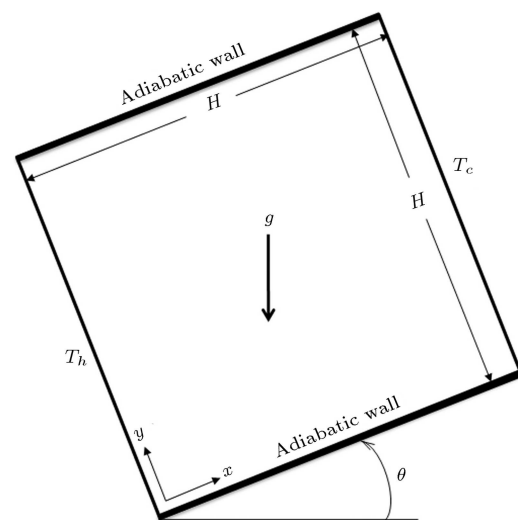


Figure 1. Schematic for physical model.

**Table 1.** Thermophysical properties of water and nanoparticles [45].

Property	Fluid phase (water)	Solid phase (SiO <sub>2</sub> )
$c_p$ (J/kgK)	4179	765
$\rho$ (kg/m <sup>3</sup> )	997.1	3970
$k$ (W/mK)	0.613	36
$\beta \times 10^{-5}$ (K <sup>-1</sup> )	21	0.63
$\alpha \times 10^{-7}$ (m <sup>2</sup> /s)	1.47	118.536
$\mu \times 10^{-4}$ (kg/ms)	8.9	—
$d_p$ (nm)	—	100

and also a volume fraction of the secondary phase. Instead of utilizing the governing equations of each phase separately, continuity, momentum and energy equations for the mixture are employed [15,17,18,23]. A nanofluid consisting of water and SiO<sub>2</sub> nanoparticles in a square inclined cavity is considered. The two sidewalls are at different constant temperatures and the others are thermally insulated.

The physical properties of the fluid are assumed constant, except for the density in the body force, which varies linearly with the temperature (Boussinesq's hypothesis). Dissipation and pressure work are neglected. Therefore, the dimensional equations for steady state mean conditions are:

Continuity equation:

$$\nabla \cdot (\rho_{\text{eff}} V_m) = 0. \quad (1)$$

Momentum equation:

$$\nabla \cdot (\rho_{\text{eff}} V_m V_m) = -\nabla P + \nabla \cdot [\tau] - \rho_{\text{eff}} \beta_{\text{eff}} (T - T_0) g + \nabla \cdot \left( \sum_{k=1}^n \phi_k \rho_k V_{\text{dr},k} V_{\text{dr},k} \right). \quad (2)$$

Energy equation:

$$\nabla \cdot \left( \sum_{k=1}^n (\rho_k c_k) \phi_k V_k T \right) = \nabla \cdot (k_{\text{eff}} \nabla T). \quad (3)$$

Volume fraction:

$$\nabla \cdot (\phi_p \rho_p V_m) = -\nabla \cdot (\phi_p \rho_p V_{\text{dr},p}), \quad (4)$$

where:

$$V_m = \frac{\sum_{k=1}^n \phi_k \rho_k V_k}{\rho_{\text{eff}}}, \quad (5)$$

$$\tau = \mu_{\text{eff}} \nabla V_m, \quad (6)$$

are the mean velocity and shear stress, respectively, and  $\phi$  is the volume fraction of phase  $k$ .

In Eq. (2),  $V_{\text{dr},k}$  is the drift velocity for the secondary phase  $k$ , i.e. the nanoparticles in the present study.

$$V_{\text{dr},k} = V_k - V_m. \quad (7)$$

The slip velocity (relative velocity) is defined as the velocity of a secondary phase ( $p$ ) relative to the velocity of the primary phase ( $f$ ):

$$V_{pf} = V_p - V_f. \quad (8)$$

The drift velocity is related to the relative velocity:

$$V_{\text{dr},p} = V_{pf} - \sum_{k=1}^n \frac{\phi_k \rho_k}{\rho_{\text{eff}}} V_{fk}. \quad (9)$$

The relative velocity is determined from Eq. (10) proposed by Manninen et al. [23], while Eq. (11), by Schiller and Naumann [24], is used to calculate the drag function,  $f_{\text{drag}}$ , as follows:

$$V_{pf} = \frac{\rho_p d_p^2}{18 \mu_f f_{\text{drag}}} \frac{(\rho_p - \rho_{\text{eff}})}{\rho_p} a, \quad (10)$$

$$f_{\text{drag}} = \begin{cases} 1 + 0.15 \text{Re}_p^{0.687} & \text{Re}_p \leq 1000 \\ 0.15 \text{Re}_p & \text{Re}_p > 1000 \end{cases} \quad (11)$$

where:

$$\text{Re}_p = \frac{d_p \rho_p |V_{pf}|}{\mu_m},$$

and acceleration  $a$  in Eq. (10) is:

$$a = g - (V_m \cdot \nabla) V_m. \quad (12)$$

The physical properties in the equations above are effective density:

$$\rho_{\text{eff}} = (1 - \phi) \rho_f + \phi \rho_p. \quad (13)$$

And effective thermal expansion coefficient [7]:

$$\beta_{\text{eff}} = \left[ \frac{1}{1 + \frac{(1-\phi)\rho_f}{\phi\rho_p}} \frac{\beta_p}{\beta_f} + \frac{1}{1 + \frac{\phi}{(1-\phi)} \frac{\rho_p}{\rho_f}} \right] \beta_f. \quad (14)$$

The effective viscosity of a fluid containing a dilute suspension of small rigid spherical particles is given by Brinkman [25]:

$$\mu_{\text{eff}} = \frac{\mu_f}{(1 - \phi)^{0.25}}. \quad (15)$$

The effective thermal conductivity of the nanofluid

restricted to spherical nanoparticles is approximated by the Maxwell-Garnetts model [26]:

$$\frac{k_{\text{eff}}}{k_f} = \frac{k_p + 2k_f - 2\phi(k_f - k_p)}{k_p + 2k_f + \phi(k_f - k_p)}. \quad (16)$$

This model is found to be appropriate for studying heat transfer enhancement using nanofluids [10–12].

The local Nusselt number of the nanofluid along the hot wall can be expressed as:

$$\text{Nu}_{\text{loc}} = \frac{Q}{Q_{\text{cond, fluid}}} = - \left( \frac{k_{\text{eff}}}{k_f} \right) \frac{\partial \theta}{\partial X}. \quad (17)$$

The average Nusselt number throughout the cavity is evaluated as:

$$\text{Nu} = \frac{1}{H} \int_0^H \text{Nu}_{\text{loc}}(y) dy. \quad (18)$$

Rayleigh and Prandtl numbers for the based fluid are given by:

$$\text{Pr} = \frac{\mu_f}{k_f}, \quad \text{Ra} = \frac{g\beta_f \Delta T H^3}{\nu_f \alpha_f}. \quad (19)$$

#### 4. Numerical procedure and validation

The system of equations above is numerically solved by a finite-volume approach [27–33] using the SIMPLE algorithm [27,34]. Central differencing is adopted for the diffusion terms and an upwind scheme is utilized for the nonlinear convective terms. The algebraic system resulting from numerical discretization is solved by TDMA (Tridiagonal Matrix Algorithm) applied in a line going through all volumes in the computational domain. Non-uniform grids in  $x$  and  $y$  directions are used for all computations [15]. To test and assess the grid independence of the solution scheme, numerical experiments are performed, as shown in Table 2. These experiments show that an unequally spaced grid mesh of  $101 \times 101$  is adequate to describe the flow and heat and mass transfer processes correctly. The absolute convergence criterion of  $(|\Omega^n - \Omega^{n-1}| < 10^{-7})$  is used for the termination of all computations, where  $\Omega(u, v, T, \phi)$  is the dependant variable in the partial

**Table 2.** Grid independency test against the Nusselt (Nu) number at  $\phi = 6\%$ ,  $\theta = 0^\circ$  and  $\text{Ra} = 10^7$ .

Grid dimension (X by Y)	Nu <sub>0</sub>
41 × 41	19.940
61 × 61	20.113
81 × 81	19.836
101 × 101	19.845
121 × 121	19.848

differential equations [15,35–42] and  $n$  is the iteration number. An under-relaxation parameter of 0.4 is used in order to obtain a stable convergence for the solution of momentum and energy equations. For the final number of grids, the computational time for each case was between 5–10 minutes. Validation of the present computer programming code has been verified for the natural convection in a square cavity in [7,43–45].

Comparison of the present results with previous work shows excellent agreement for average Nusselt number, as shown in Table 3. Moreover, to demonstrate the precision of the model, results are compared with those obtained by Jahanshahi et al. [46]. They studied the natural convection of a water-SiO<sub>2</sub> nanofluid using two different thermal conductivity models. In the first method, they employed a set of experimental data for thermal conductivity of the nanofluid and, in the second, they calculated the thermal conductivity from the equation proposed by Hamilton and Crosser [47]. As shown in Figure 2, the mixture model results are in much better agreement with the solution based on experimental thermal conductivity [15]. It is an interesting feature of the mixture model, especially for high Rayleigh numbers, since higher Rayleigh numbers could result in non-uniform distribution, for which the single phase approach would no longer be precise.

#### 5. Results and discussion

Numerical analysis using a two-phase mixture model has been carried out to investigate the effects of

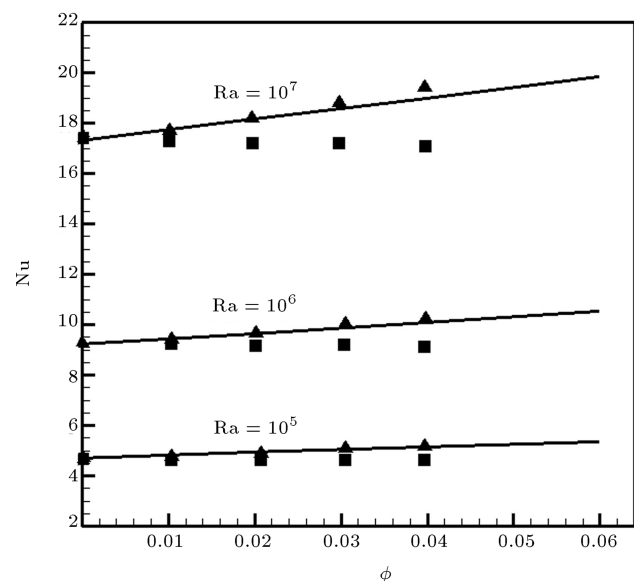


**Figure 2.** Comparison of the present results (solid lines) with that of [46]. (▲) represents the data obtained based on the experimental thermal conductivity, and (■) shows the results calculated by Hamilton and Crosser conductivity model [47].

**Table 3.** Comparison of the Nusselt number for different Rayleigh numbers.

Ra	Present	Khanafer et al. [7]	De Vahl Davis [43]	Fusegi et al. [44]	Barakos and Mitsoulis [45]
$\frac{10^3}{Nu}$	1.118	1.118	1.118	1.105	1.114
$U_{max}$ at $(Y/H)$	0.138 (0.808)	0.137 (0.812)	0.136 (0.813)	0.132 (0.833)	0.153 (0.806)
$V_{max}$ at $(X/L)$	0.140 (0.181)	0.139 (0.173)	0.138 (0.178)	0.131 (0.200)	0.155 (0.181)
$\frac{10^4}{Nu}$	2.244	2.245	2.243	2.302	2.245
$U_{max}$ at $(Y/H)$	0.193 (0.819)	0.192 (0.827)	0.192 (0.823)	0.201 (0.817)	0.193 (0.818)
$V_{max}$ at $(X/L)$	0.234 (0.121)	0.233 (0.123)	0.234 (0.119)	0.225 (0.117)	0.234 (0.119)
$\frac{10^5}{Nu}$	4.519	4.522	4.519	4.646	4.510
$U_{max}$ at $(Y/H)$	0.132 (0.850)	0.131 (0.854)	0.153 (0.855)	0.147 (0.855)	0.132 (0.859)
$V_{max}$ at $(X/L)$	0.259 (0.063)	0.258 (0.065)	0.261 (0.066)	0.247 (0.065)	0.258 (0.066)
$\frac{10^6}{Nu}$	8.817	8.826	8.799	9.012	8.806
$U_{max}$ at $(Y/H)$	0.077 (0.850)	0.077 (0.854)	0.079 (0.850)	0.084 (0.856)	0.077 (0.859)
$V_{max}$ at $(X/L)$	0.263 (0.035)	0.262 (0.039)	0.262 (0.038)	0.259 (0.033)	0.262 (0.039)

Rayleigh number and inclination angle on a SiO<sub>2</sub>-water nanofluid filling a two dimensional inclined square enclosure. The enclosure is differentially heated and the other two opposite walls are adiabatic. Calculations are made for various values of volume fraction of nanoparticle ( $0 \leq \phi \leq 6\%$ ), inclination angles ( $-60^\circ \leq \theta \leq 60^\circ$ ) and Rayleigh numbers ( $10^3 \leq Ra \leq 10^7$ ).

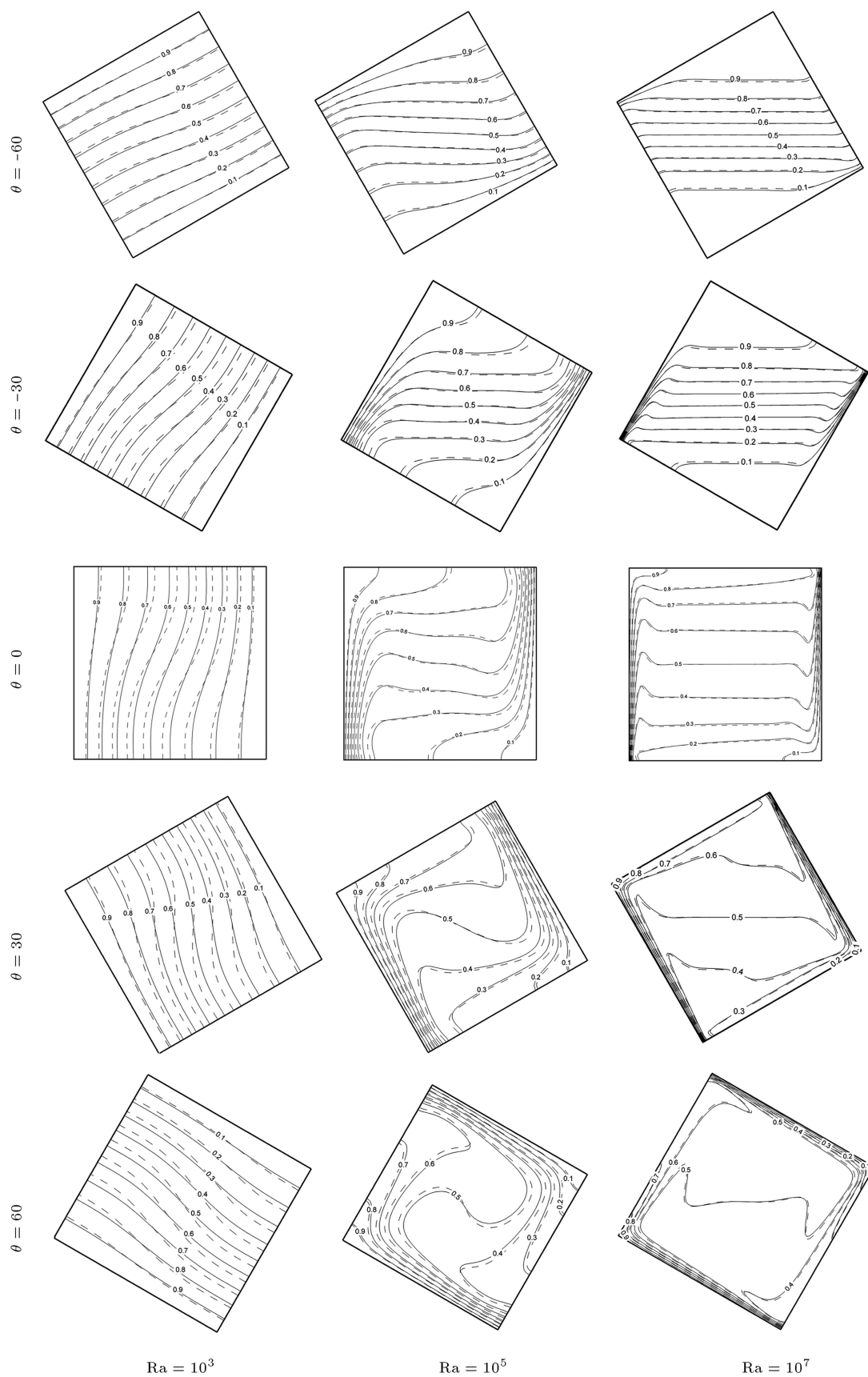
Figure 3 illustrates the isotherms at various inclination angles and Rayleigh numbers for both the pure fluid and nanofluid, with  $\phi = 6\%$ . In general, as Rayleigh number increases, more deflection occurs in isotherms. This is due to the convection dominated mechanism for heat transfer at high Rayleigh number compared to the conduction mechanism at lower Rayleigh number. Also, isotherms indicate that inclination angle has no specific effect on temperature contours for low Rayleigh number, where the conduction is more pronounced. At higher Rayleigh number, when  $\theta = -60, -30$ , the isotherms are stratified in the vertical direction, because the hot wall is located above the cold. But, with increase of  $\theta$ , thermal stratification reduces considerably. Effects of volume fraction on isotherms is also depicted in Figure 3 for different  $\theta$  and Ra. As can be seen, at the lower Rayleigh number, the solid concentration has more effect on increasing heat penetration. In fact, the variation of thermal boundary layer thickness is related to the thermal conductivity of the nanofluid.

Figure 4 shows the effects of Rayleigh number on streamlines for  $\phi = 60\%$  at various inclination angles. The figure presents a comparison between nanofluid (solid lines —) and pure fluid (dashed lines - - -).

A singular cell is formed at low Rayleigh number and the shape of the main cell is circular as a dominant characteristic of the fluid flow. It is observed that the strength of circulation increases rapidly with increase in Rayleigh number. This is obviously due to an increase in buoyancy, as viscosity and density remain the same for a particular  $\phi$ . Also, the thickness of the velocity boundary layer near the walls decreases and, hence, the stagnant core zone increases with an increase in Rayleigh number. As shown in the figure, the shape of the cell becomes ellipsoidal with an increase in Rayleigh number; the central vortex tends to become elliptic for  $Ra = 10^5$  and, eventually, breaks up into three vortices for a Rayleigh number of  $Ra = 10^7$ . The addition of nanoparticles affects the diameter of the cell. It is observed that the shape of the main cell is sensitive to the inclination angle and addition of nanoparticles.

Using a two-phase approach gives significant information on nanoparticle distribution.

Figure 5 depicts nanoparticle distribution based on  $(\phi_P - \phi_{P_0}) \times 10^3$  for various inclination angles and Rayleigh numbers. Nanoparticle distribution becomes more severe for higher Rayleigh numbers. This increase in the variation of nanoparticle concentration shows no uniform properties of nanofluid in the cavity at higher Rayleigh numbers. At lower Rayleigh numbers, particle distribution is fairly uniform and a single phase approach could be well adopted. The effect of acceleration  $g$  (gravity) is noticeable on the concentration of nanoparticles at the bottom of the cavity (nanoparticle accumulation) for different inclination angles.



**Figure 3.** Isotherms for various inclination angles and Rayleigh numbers for pure fluid (dashed lines - - -) and nanofluid with  $\phi = 6\%$  (solid lines ———).

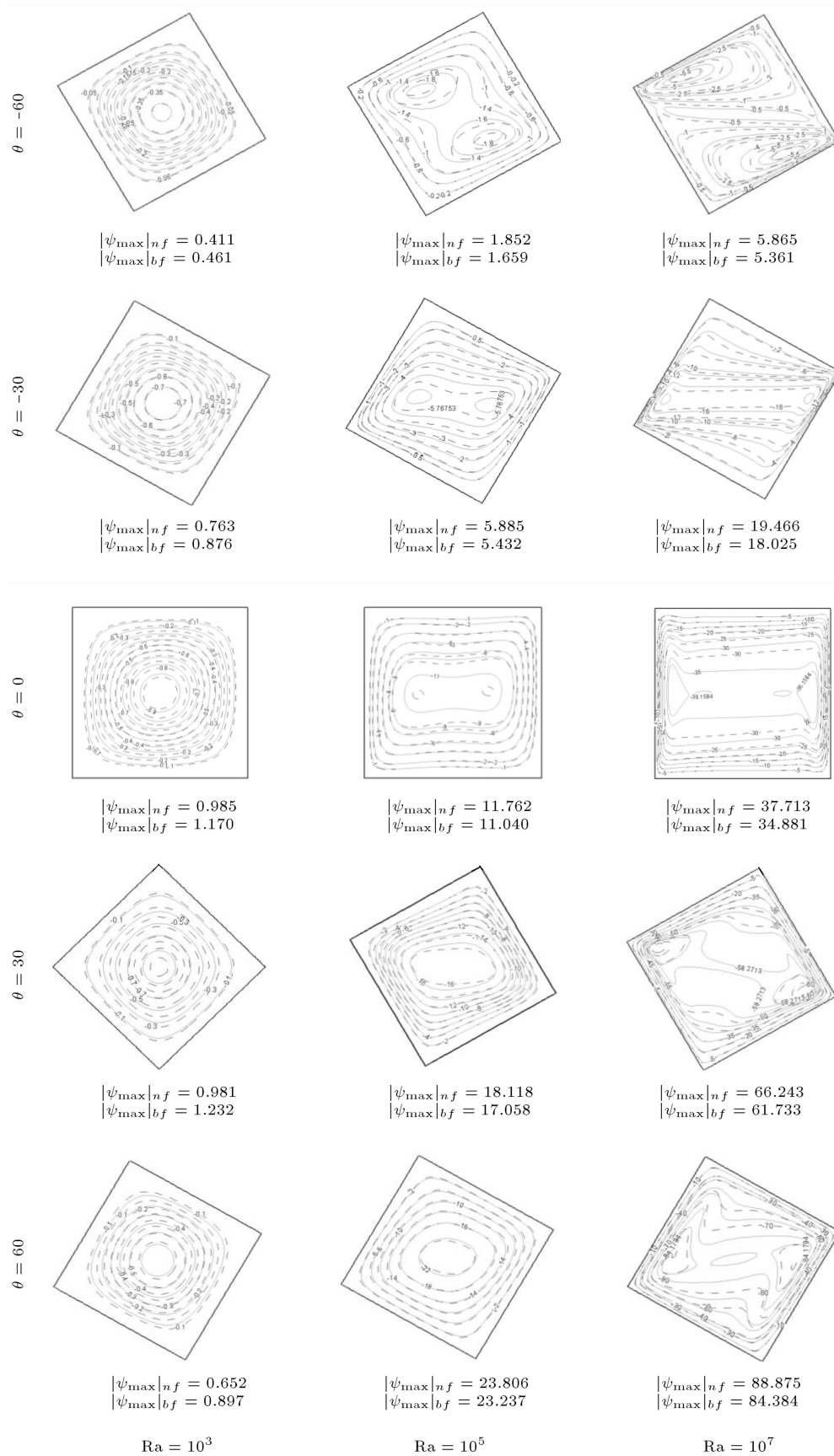


**Figure 4.** Stream lines for various inclination angles and Rayleigh numbers for pure fluid (dashed lines - - -) and nanofluid with  $\phi = 6\%$  (solid lines ———).



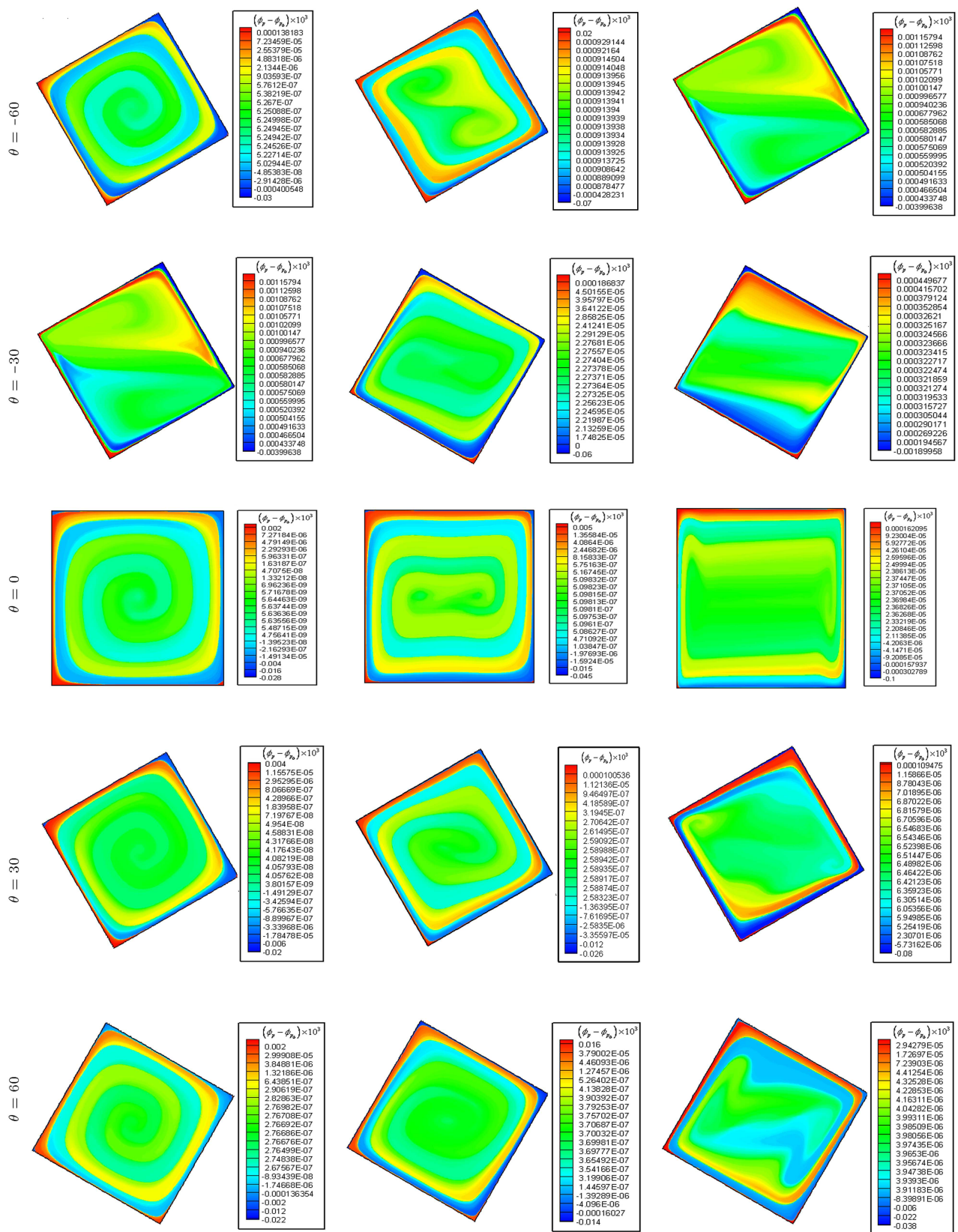


**Figure 5.** Contours of nanoparticles distribution for various inclination angles and Rayleigh numbers at  $\phi = 6\%$ .



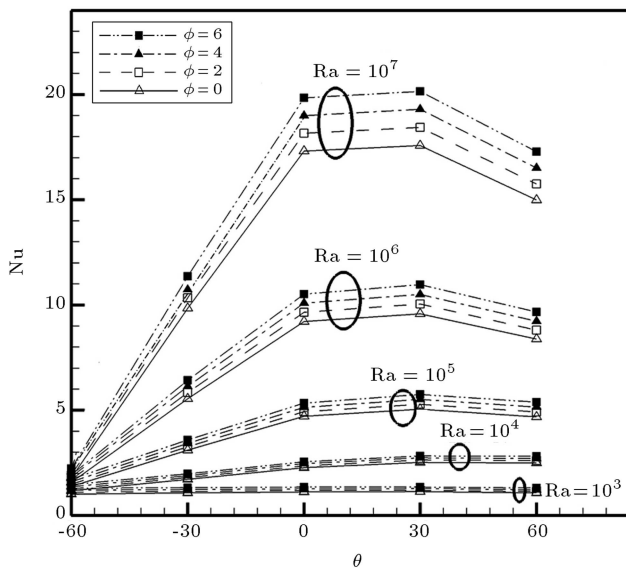


**Figure 6.** Variation of average Nusselt number for various values of volume fraction ( $\phi$ ) and inclination angles ( $\theta$ ) at different Rayleigh numbers.

Figure 6 comprehensively presents the effects of volume fraction, Rayleigh number and inclination angle on heat transfer. As seen, Nusselt number increases with the growth of volume fraction at any inclination angle. Heat transfer enhances with an increment in Rayleigh number for any specific inclination angle and volume fraction. Maximum heat transfer occurs at an angle of  $30^\circ$ . This is due to the increase of flow velocity at this angle, while the Nusselt number has its lowest amount at an inclination angle of  $-60^\circ$ , due to the low velocity encountered at this angle. Also, the figure shows that the conduction regime prevailed for  $Ra = 1000$  and, then, the mean Nusselt number started to deviate from the value of  $Nu \cong 1$ .

## 6. Conclusions

Natural convection of a nanofluid consisting of water and  $\text{SiO}_2$  in an inclined square enclosure has been studied numerically. A two-phase mixture model has been used to investigate, numerically, the effect of Rayleigh number, inclination angle and volume fraction of nanoparticles. Results have clearly indicated that the addition of  $\text{SiO}_2$  nanoparticles has produced a remarkable enhancement to heat transfer, with respect to that of pure fluid. The effect of nanoparticle concentration on Nusselt number is more pronounced at low Rayleigh numbers than at high Rayleigh numbers; this is related to the conduction dominated mechanism for heat transfer at low Rayleigh numbers compared to convection mechanisms at higher Rayleigh numbers. The inclination angle of the enclosure is proposed as a control parameter for fluid flow and heat transfer. It is found that lower heat transfer is formed for  $-60^\circ$ .

The effects of inclination angle on the percentage of heat transfer enhancement become insignificant at low Rayleigh numbers. Unlike the single phase model, the mixture model calculates the distribution of nanoparticle concentration so that obtained values of Nusselt number are closer to experimental data, especially at higher Rayleigh numbers. This shows that the mixture model is better able to model the physics of nanofluids.

## Nomenclature

$C_p$	Specific heat (J/kg K)
$d_p$	Nanoparticle diameter (nm)
$d_f$	Molecular diameter of base fluid
$g$	Gravitational acceleration ( $\text{m s}^{-2}$ )
$Ra$	Rayleigh number ( $= \frac{g\beta_f\Delta TH^3}{\nu_f\alpha_f}$ )
$K$	Thermal conductivity (W/m K)
$Nu$	Average Nusselt number
$P$	Pressure (Pa)
$Pr$	Prandtl number ( $= \frac{\mu_f}{k_f}$ )
$T$	Temperature (K)
$V$	Velocity ( $\text{m s}^{-1}$ )
$x, y$	Cartesian coordinates (m)

## Greek letters

$\alpha$	Thermal diffusivity ( $= \frac{k}{\rho c_p}$ )
$\beta$	Volumetric expansion coefficient ( $\text{K}^{-1}$ )
$\theta$	Angular coordinate
$\phi$	volume fraction
$\mu$	Dynamic viscosity ( $\text{N s m}^{-2}$ )
$\nu$	Kinematic viscosity ( $= \frac{\mu}{\rho} (\text{m}^2 \text{s}^{-1})$ )
$\rho$	Density ( $\text{kg m}^{-3}$ )

## Subscripts

$b$	Bulk
$dr$	Drift
$eff$	Effective
$f$	Base fluid
$k$	Summation index
$m$	Mixture
$p$	Particle
$h$	Hot wall
$c$	Cold wall

## References

1. Maxwell, J.C., *Electricity and Magnetism*, Clarendon Press, Oxford, UK (1873).

2. Choi, S.U.S. "Enhancing thermal conductivity of fluid with nanoparticles, developments and applications of non-Newtonian flow", *ASME, FED 231/MD*, **66**, pp. 99-105 (1995).
3. Xuan, Y.M. and Roetzel, W. "Conceptions for heat transfer correlation of nanofluids", *Int. J. Heat Mass Trans.*, **43**, pp. 3701-3707 (2000).
4. Keblinski, P., Phillpot, S.R., Choi, S.U.S. and Eastman, J.A. "Mechanisms of heat flow in suspensions of nano-sized particles (nanofluid)", *Int. J. Heat Mass Trans.*, **45**, pp. 855-863 (2002).
5. Wen, D. and Ding, Y. "Experimental investigation into convective heat transfer of nanofluids at the entrance region under laminar flow conditions", *Int. J. Heat Mass Trans.*, **47**, pp. 5181-5188 (2004).
6. Anoop, K.B., Sundararajan, T. and Das, S.K. "Effect of particle size on the convective heat transfer in nanofluid in the developing region", *Int. J. Heat Mass Trans.*, **52**, pp. 735-743 (2009).
7. Khanafer, K., Vafai, K. and Lightstone, M. "Buoyancy-driven heat transfer enhancement in a two dimensional enclosure utilizing nanofluids", *Int. J. Heat Mass Trans.*, **46**, pp. 3639-3653 (2003).
8. Abu-Nada, E. and Oztop, H.F. "Effects of inclination angle on natural convection in enclosures filled with Cu-water nanofluid", *Int. J. Heat and Fluid Flow*, **30**, pp. 669-678 (2009).
9. Ho, C.J., Chen, M.W. and Li, Z.W. "Numerical simulation of natural convection of nanofluid in a square enclosure: Effects due to uncertainties of viscosity and thermal conductivity", *Int. J. Heat Mass Trans.*, **51**(17-18), pp. 4506-4516 (2008).
10. Oztop, H.F. and Abu-Nada, E. "Numerical study of natural convection in partially heated rectangular enclosures filled with nanofluids", *Int. J. Heat Fluid Flow*, **29**(5), pp. 1326-1336 (2008).
11. Palm, S., Roy, G. and Nguyen, C.T. "Heat transfer enhancement with the use of nanofluids in a radial flow cooling system considering temperature dependent properties", *Appl. Therm. Eng.*, **26**, pp. 2209-2218 (2006).
12. Saleh, H., Roslan, R. and Hashim, I. "Natural convection heat transfer in a nanofluid-filled trapezoidal enclosure", *Int. J. Heat and Mass Trans.*, **54**, pp. 194-201 (2011).
13. Kumar Santra, A., Sen, S. and Chakraborty, N. "Study of heat transfer augmentation in a differentially heated square cavity using copper-water nanofluid", *Int. J. Therm. Sci.*, **47**, pp. 1113-1122 (2008).
14. Ghasemi, B. and Aminossadati, S.M. "Natural convection heat transfer in an inclined enclosure filled with a water-Cuo nanofluid", *Numer. Heat Trans.; Part A: Appl.*, **55**, pp. 807-823 (2009).
15. Alinia, M., Ganji, D.D. and Gorji-Bandpy, M. "Numerical study of mixed convection in an inclined two sided lid driven cavity filled with nanofluid using two-phase mixture model", *Int. Comm. Heat and Mass Trans.*, **38**, pp. 1428-1435 (2011).
16. Koo, J. and Kleinstreuer, C. "Laminar nanofluid flow in microheat-sinks", *Int. J. Heat Mass Trans.*, **48**, pp. 2652-2661 (2005).
17. Akbarinia, A. and Behzadmehr, A. "Numerical study of laminar mixed convection of a nanofluid in a horizontal curved tube", *Appl. Therm. Eng.*, **27**, pp. 1327-1337 (2007).
18. Akbari, M. and Behzadmehr, A. "Developing laminar mixed convection of a nanofluid in a horizontal tube with uniform heat flux", *Int. J. Num. Meth. Heat Fluid Flow*, **17**, pp. 566-586 (2007).
19. Ding, Y. and Wen, D. "Particle migration in a flow of nanoparticle suspensions", *Powder Tech.*, **149**, pp. 84-92 (2005).
20. Xuan, Y.M. and Li, Q. "Heat transfer enhancement of nanofluids", *Int. J. Heat Fluid Flow*, **21**, pp. 58-64 (2000).
21. Behzadmehr, A., Saffar-Avval, M. and Galanis, N. "Prediction of turbulent forced convection of a nanofluid in a tube with uniform heat flux using a two-phase approach", *Int. J. Heat Fluid Flow*, **28**, pp. 211-219 (2007).
22. Lotfi, R., Saboohi, Y. and Rashidi, A.M. "Numerical study of forced convective heat transfer of nanofluids: Comparison of different approaches", *Int. Comm. in Heat and Mass Trans.*, **37**, pp. 74-78 (2010).
23. Manninen, M., Taivassalo, V. and Kallio, S. "On the mixture model for multiphase flow", *Tech. Resea. Cent. of Finland, VTT Pub.*, **288**, pp. 9-18 (1996).
24. Schiller, L. and Naumann, A. "A drag coefficient correlation", *Z. Ver. Deutsch. Ing.*, **77**, pp. 318-320 (1935).
25. Brinkman, H.C. "The viscosity of concentrated suspensions and solutions", *J. Chem. Phys.*, **20**, pp. 571-581 (1952).
26. Maxwell, J., *A Treatise on Electricity and Magnetism*, 2nd Ed. Oxf. Uni. Pre., Cambridge, UK, pp. 435-441 (1904).
27. Ghasemi, E., Soleimani, S. and Bayat, M. "Control volume based finite element method study of nanofluid natural convection heat transfer in an enclosure between a circular and a sinusoidal cylinder", *Int. J. of Nonlinear. Sci. and Numer. Sim.*, **14**(7-8), pp. 521-532 (2013).
28. Ghasemisahebi, E., *Entropy Generation in Transitional Boundary Layers*, LAP LAMBERT Aca. Pub. (2013).
29. Ghasemi, E., McEligot, D.M., Nolan, K., Crepeau, J., Tokuhito, A. and Budwig, R.S. "Entropy generation in transitional boundary layer region under the influence of freestream turbulence using transitional RANS models and DNS", *Int. Comm. Heat. Mass. Trans.*, **41**, pp. 10-16 (2013).
30. Ghasemi, E., Soleimani, S. and Bararnia, H. "Natural convection between a circular enclosure and an elliptic cylinder using control volume based finite element

- method", *Int. Comm. in Heat and Mass Trans.*, **39**, pp. 1035-1044 (2012).
31. Soleimani, S., Ganji, D.D., Gorji, M., Bararnia, H. and Ghasemi, E. "Optimal location of a pair heat source-sink in an enclosed square cavity with natural convection through PSO algorithm", *Int. Comm. in Heat and Mass Trans.*, **38**, pp. 652-658 (2011).
  32. Taeibi-Rahni, M., Ramezanizadeh, M., Ganji, D.D., Darvan, A., Ghasemi, E., Soleimani, S. and Bararni, H. "Comparative study of large eddy simulation of film cooling using a dynamic global-coefficient subgrid scale eddy-viscosity model with RANS and Smagorinsky modeling", *Int. Comm. in Heat and Mass Trans.*, **38**, pp. 659-667 (2011).
  33. Taeibi-Rahni, M., Ramezanizadeh, M., Ganji, D.D., Darvan, A., Ghasemi, E., Soleimani, S. and Bararni, H. "Large-eddy simulations of three dimensional turbulent jet in a cross flow using a dynamic subgrid-scale eddy viscosity model with a global model coefficient", *World Appl. Sci. J.*, **9**(10), pp. 1191-1200 (2010).
  34. Patnkar, S.V., *Numerical Heat Transfer and Fluid Flow*, Hemisphere Pub., New York (1980).
  35. Ganji, D.D., Bararnia, H., Soleimani, S. and Ghasemi, E. "Analytical solution of the magneto-hydrodynamic flow over a nonlinear stretching sheet", *Mod. Phy. Lett. B.*, **23**, pp. 2541-2556 (2009).
  36. Jalaal, M., Ghasemi, E., Ganji, D.D., Bararnia, H., Soleimani, S., Nejad, G.M. and Esmailpour, M. "Effect of temperature-dependency of surface emissivity on heat transfer using the parameterized perturbation method", *Ther. Sci.*, **15**(suppl. 1), pp. 123-125 (2011).
  37. Ghasemi, E., Soleimani, S., Bararnia, H. and Domairry, G. "Influence of uniform suction/injection on heat transfer of MHD Hiemenz flow in porous media", *J. of Eng. Mech., ASCE*, **138**(1), pp. 82-88 (2012).
  38. Soleimani, S., Ganji, D.D., Ghasemi, E., Jalaal, M. and Bararnia, H. "Meshless local RBF-DG for 2-D heat conduction: A comparative study", *The. Sci.*, **15**(suppl. 1), pp. 117-121 (2011).
  39. Bararnia, H., Ghasemi, E., Soleimani, S., Ghotbi, A.R. and Ganji, D.D. "Solution of the Falkner-Skan wedge flow by HPM-Pade' method", *Adv. in Eng. Soft.*, **43**, pp. 44-52 (2012).
  40. Ghasemi, E., Bayat, M. and Bayat, M. "Visco-elastic MHD flow of Walters liquid b fluid and heat transfer over a non-isothermal stretching sheet", *Int. J. Phys. Sci.*, **6**(21), pp. 5022-5039 (2011).
  41. Kutanaei, S.S., Ghasemi, E. and Bayat, M. "Mesh-free modeling of two-dimensional heat conduction between eccentric circular cylinders", *Int. J. Phy. Sci.*, **6**(16), pp. 4044-4052 (2011).
  42. Seyyedi, S.M., Soleimani, S., Ghasemi, E., Ganji, D.D., Gorji-Bandpy, M. and Bararnia, H. "Numerical investigation of laminar mixed convection in a cubic cavity by MRT-LBM: Effects of the sliding direction", *Num. Heat Trans. Part A: Appl.*, **63**(4), pp. 285-304 (2013).
  43. De Vahl Davis, G. "Natural convection of air in a square cavity, a benchmark numerical solution", *Int. J. Numer. Meth. Fluids*, **3**, pp. 249-264 (1962).
  44. Fusegi, T., Hyun, J.M., Kuwahara, K. and Farouk, B. "A numerical study of three-dimensional natural convection in a differentially heated cubical enclosure", *Int. J. Heat Mass Trans.*, **34**, pp. 1543-1557 (1991).
  45. Barakos, G. and Mitsoulis, E. "Natural convection flow in a square cavity revisited: laminar and turbulent models with wall functions", *Int. J. Num. Methods Fluids*, **18**, pp. 695-719 (1994).
  46. Jahanshahi, M., Hosseinzadeh, S.F., Alipanah, M., Dehghani, A. and Vakilinejad, G.R. "Numerical simulation of free convection based on experimental measured conductivity in a square cavity using water/SiO<sub>2</sub> nanofluid", *Int. Comm. Heat and Mass Trans.*, **37**, pp. 687-694 (2010).
  47. Hamilton, R.L. and Crosser, O.K. "Thermal conductivity of heterogeneous two component systems", *I&EC Fund.*, **1**(3), pp. 187-191 (1962).

## Biographies

**Mohammad Alinia** received his BSc degree from school of Mechanical Engineering in Thermo-fluid subfield at Mazandaran University and his MSc degree in Energy Conversion subfield from school of Mechanical Engineering at Babol Noshirvani University of Technology. His research interests are computational fluid dynamics, multiphase flow, heat transfer and mass transfer.

**Mofid Gorji-Bandpy** is a Professor of Mechanical Engineering Department at Babol Noshirvani University of Technology, Babol, Iran. He received his PhD in Mechanical Engineering from University of Wales College of Cardiff. His research work concerns fluid mechanics, turbomachinery and all of the hydro-engineering subjects, renewable energy, water distribution networks, mechanics and thermodynamics of propulsion systems and internal combustion chamber.

**Davood Domiri Ganji** is Associate Professor of Mechanical Engineering Department at Babol Noshirvani University of Technology, Babol, Iran. He received his PhD in Mechanical Engineering from Tarbiat Modares University. His research interests are nonlinear science in engineering, CFD, inverse problems and spray modeling.

**Soheil Soleimani Kutanaei** received his BSc degree from school of Mechanical Engineering in Thermo-fluid subfield at Mazandaran University and his MSc degree in Energy Conversion subfield from school of Mechanical Engineering at Babol Noshirvani University of Technology. He is a PhD student at the Department of

mechanical and materials of the Florida International University (FIU). His main research interests are computational fluid dynamics and computational physics, Turbulence reacting flow, heat and mass transfer and multiphase flow in meso and micro scales and heat transfer optimization.

**Esmail Ghasemi Sahebi** received his BS in Mechanical Engineering in Thermo-fluid subfield at Mazandaran University. He received his master degree in mechanical engineering from University of Idaho. He is currently a PhD student at Florida International

University (FIU). His main research interests are computational fluid dynamic and computational physics, turbulent flow modeling, heat transfer and entropy generation.

**Ali Darvan** received his MSc degree in Energy Conversion subfield from school of Mechanical Engineering at Islamic Azad University of Science and Research of Tehran. He is currently a PhD student at Martin Luther University. His research area is modeling and numerical computation of droplet behavior in spray drying equipment.